Materials Science Forum Vols. 170-172 (1994) pp. 47-52

EXPERIMENTAL AND NUMERICAL INVESTIGATIONS OF SUPERPLASTIC DEFORMATION MECHANISMS

N. Chandra, K. Murali and H. Garmestani

Department of Mechanical Engineering, FAMU/FSU College of Engineering,
Florida A&M University, Florida State University, Tallahassee, FL 32316-2175, USA

ABSTRACT

Experimental and numerical investigations of superplastic deformation are being carried out in order to understand the underlying mechanisms of deformation in low (conventional) and high strain-rate ranges. The experimental analysis consists of analyzing the microstructure using Backscattered Kikuchi Diffraction (BKD) method and relating it to the various mechanisms of superplastic deformation. The numerical investigation consists of developing a micromechanical model of superplastic deformation from the constituent grain level to the level of the polycrystalline aggregate. This model uses the self-consistent method to evaluate the grain to grain variation of stress during superplastic deformation. It is applied to statically recrystallized 7475 aluminum alloy and dynamically recrystallizing SUPRAL and the influence of temperature on the flow stress vs. strain rate behavior is successfully predicted.

INTRODUCTION

The advent of high strain rate superplasticity (HSRS) where superplasticity is observed at strain rates of 10^{-1} to 10^{2} s^{-1} has led to renewed interest in superplasticity by automotive, architectural, and other sheet-metal industries, as HSRS requires shorter forming time leading to reduced cost. HSRS has been reported in the following materials: a) powder metallurgy, pseudo single phase alloys such as 7475 Al-Zr alloy, b) mechanically alloyed alloys such as IN 9021 and IN90211, and c) metal matrix composites such as Al 2124, 6061, and 7064 reinforced with α/β Si_3N_4 or SiC. Different combinations of matrix and reinforcement materials either lead to or do not lead to HSRS. The micromechanics of HSRS is presently not clearly understood; and even in low strain rate superplastic flow the role of various accommodation mechanisms is unclear. Modeling can be used to study the deformation mechanisms causing HSRS and to predict the presence or absence of HSRS in existing and new materials. Towards this end, experimental and numerical investigations of superplastic deformation are being carried out.

In the experimental investigation, which is in its preliminary stages, we use BKD method to determine the crystallographic orientation of individual grains and evaluate ODF and MDF (orientation and misorientation distribution functions) in superplastic specimens with increasing levels of strain, both uniaxial and biaxial. With these, it would be possible to correlate the changes in microtextural quantities (overall intensity, strength of specific texture components) with dislocation, diffusion, and grain boundary sliding (GBS) mechanisms of superplastic deformation. Fig. 1 shows a typical BKD pattern in which the poles have been identified. The results have not been fully analyzed at this stage.

In the numerical investigation, we have developed a micromechanical model of superplastic deformation based on the underlying mechanisms. The most important among them, GBS, has been shown to account for essentially all the deformation under optimum superplastic conditions [1]. It is also recognized that GBS is accommodated by diffusional and dislocation mechanisms active within the grains and their boundaries. Most of the existing models for superplasticity relate the strain rate of the accommodation processes of GBS to the macroscopically measured strain rate. We conform to this approach in our model and consider accommodation due to diffusional flow and dislocation movement at the grain level. The model derives the superplastic strain of the aggregate from the level of its constituent grains. It uses the self-consistent method to evaluate the grain to grain variation of stress during superplastic deformation. The crystallographic structure of the material and the corresponding slip systems are used in modeling the deformation in a grain, similar to Murali and Weng's [2] unified theory of creep and strain-rate sensitivity of polycrystals. It is used to predict the influence of temperature on the flow stress vs. strain rate behavior of superplastic materials.

SUPERPLASTIC DEFORMATION MECHANISMS

Table 1 of a paper by Sherby and Wadsworth [3] lists the various mechanism-based deformation models for superplasticity. It is clear from the table that the existing models of superplasticity relate the macroscopically measured strain rate to the strain rate of the diffusional and/or dislocational accommodation mechanisms by using constant proportionality factors. This relationship can be expressed as:

$$\dot{\epsilon}^{sp} = K \cdot \dot{\epsilon}_{acc} \tag{1}$$

We adopt this approach and evaluate the accommodation strain rate $\dot{\epsilon}_{acc}$ due to lattice and grain boundary diffusional flow and dislocation movement. The macroscopic strain rate, $\dot{\epsilon}^{sp}$, is proportional to the sum of the strain rates of these processes.

$$\dot{\epsilon}^{sp} = K \cdot (\dot{\epsilon}'_{diff.} + \dot{\epsilon}'_{disloc.}) = \dot{\epsilon}_{diff.} + \dot{\epsilon}_{disloc.} \tag{2}$$

The proportionality factor K is built into the equations for $\dot{\epsilon}_{diff.}$ and $\dot{\epsilon}_{disloc.}$.

In our micromechanical model, we derive the superplastic behavior of bulk material from the grain level. At this level, dislocation movement is modeled as glide of dislocations on the slip plane. Thus, $\dot{\epsilon}_{disloc.}$ is controlled by the resolved shear stress τ acting on a slip plane along the slip direction, and its constitutive equation can be written as

$$\overset{(k)}{\dot{\gamma}}_{disloc.} = a_s \frac{1}{T} exp\left(\frac{-Q_L}{RT}\right) (\overset{(k)}{\tau})^n \tag{3}$$

Here, Q_L is the activation energy of lattice diffusion, T is the absolute temperature, and R is the universal gas constant. a_s and n are material constants which are determined from experimental superplastic deformation data.

Diffusional flow occurs as a result of the diffusion of atoms from one grain boundary to another which is subjected to a higher stress. The resolved normal stress σ_n acting on a slip plane has been found by Weertman [4] to direct diffusion of atoms and vacancies. Thus, $\dot{\epsilon}_{diff.}$ is controlled by σ_n and is given by the following equation:

$$\overset{(k)}{\dot{\epsilon}}_{diff.} = a_l \frac{1}{T} exp\left(\frac{-Q_L}{RT}\right) \overset{(k)}{\sigma_n} + a_b \frac{1}{T} exp\left(\frac{-Q_B}{RT}\right) \overset{(k)}{\sigma_n} \tag{4}$$

The first term represents lattice diffusion and the second term represents grain boundary diffusion. Here, Q_B is the activation energy of grain boundary diffusion, and a_l and a_b are material constants which will be determined from experimental superplastic deformation data. The proportionality factor K of equation (1) is contained within the material constants a_l, a_b and a_s.

The resolved shear stress acting on a slip system $\overset{(k)}{\tau}$ is given by

$$\overset{(k)}{\tau} = \overset{(k)}{\nu_{ij}} \sigma_{ij} \quad \text{where} \quad \overset{(k)}{\nu_{ij}} = \frac{1}{2}(b_i n_j + b_j n_i) \tag{5}$$

Here, σ_{ij} is the local stress field in the considered grain, and b_i and n_i are the slip direction and slip plane normals of the considered slip system. The resolved normal stress can be calculated as shown by Weertman in 1965 [4] using the deviatoric component of the local stress σ'_{ij} as follows:

$$\overset{(k)}{\sigma_n} = \overset{(k)}{\mu_{ij}} \sigma'_{ij}, \quad \text{where} \quad \mu_{ij} = b_i b_j \tag{6}$$

Once the strain rates of all the slip systems are calculated from the constitutive equations (3) and (4), the superplastic strain-rate components of the grain follow from

$$\dot{\epsilon}_{ij}^{sp} = \sum_k \left(\overset{(k)}{\mu_{ij}} - \frac{1}{3}\delta_{ij} \right) \overset{(k)}{\dot{\epsilon}}_{diff.} + \sum_k \overset{(k)}{\nu_{ij}} \overset{(k)}{\dot{\gamma}}_{disloc.} \tag{7}$$

POLYCRYSTALLINE MODEL

The crystal structure of the material determines the slip systems that are present. The micromechanical theory is then applied from the level of slip systems in each grain of a polycrystal. The three dimensional polycrystal model consists of 216 grains with different orientations; they are obtained by rotating a basic crystal, aligned along the material axes, first about the x_3 axis, then about the x_2 axis and finally about the x_1 axis. Due to the cubic symmetry, the rotation about each axis is taken to start from 0^o and end at 75^o, with an increment of 15^o, leading to the required $6 \times 6 \times 6 = 216$ orientations.

During superplastic deformation, stress distribution inside a polycrystal is highly heterogeneous primarily due to the variation in grain orientation. Therefore, the local stress σ_{ij} needed to calculate the resolved shear and normal stresses in equations (3) and (4) respectively, generally differs from the externally applied stress $\bar{\sigma}_{ij}$. The self-consistent relation of Budiansky and Wu [5], written in the incremental form, can reasonably account for the stress redistribution among the constituent grains. In the application of the self-consistent relation, each grain is treated as an inclusion in the matrix of the aggregate.

If the incremental superplastic strain of a grain over a time increment dt is denoted by $d\epsilon_{ij}^{sp}$, and that of the aggregate by the corresponding barred (averaging) quantity $d\bar{\epsilon}_{ij}^{sp}$, the incremental stress variation of a grain is $d\sigma_{ij}$ given by the self-consistent relation

$$d\sigma_{ij} = d\bar{\sigma}_{ij} - 2\mu(1-\beta)(d\epsilon_{ij}^{sp} - d\bar{\epsilon}_{ij}^{sp}) \tag{8}$$

when the grain is assumed to be spherical and isotropic. In this equation, $d\bar{\sigma}_{ij}$ is the applied incremental stress, and μ is the shear modulus, and in terms of Poisson's ratio ν, $\beta = (2/15) \cdot (4 - 5\nu)/(1-\nu)$. The incremental superplastic strain of a grain is given by $d\epsilon_{ij}^{sp} = \dot{\epsilon}_{ij}^{sp} dt$. Once $d\epsilon_{ij}^{sp}$ is determined for all the grains, the incremental superplastic strain of the polycrystalline aggregate can be calculated from the orientational average which is the numerical average of the incremental superplastic strains of all the grains.

We are mainly interested in determining the flow stress vs. strain rate behavior of materials while undergoing superplastic deformation. This is done by obtaining the stress-strain curves under several strain rates and then extracting the flow stress information from them. The stress-strain behavior under a constant total strain-rate $\dot{\bar{\epsilon}}_{ij}$ can be calculated incrementally as follows. The total strain-rate is the sum of the elastic and plastic strain-rates. For a given time increment, the elastic strain can be calculated from

$$d\bar{\epsilon}_{ij}^{e} = d\bar{\epsilon}_{ij}^{t} - d\bar{\epsilon}_{ij}^{sp} \tag{9}$$

which in turn provides the macroscopic stress increment $d\bar{\sigma}_{ij}$ from the constitutive equation

$$d\bar{\sigma}_{ij} = C_{ijkl} d\bar{\epsilon}_{kl}^{e} = 2\mu d\bar{\epsilon}_{ij}^{e} + \lambda\delta_{ij} d\bar{\epsilon}_{kk}^{e} \tag{10}$$

This incremental procedure is repeated to generate the entire stress-strain curve of the polycrystal till a given strain is reached. In this procedure, $d\bar{\epsilon}_{ij}^{sp}$ is obtained using (7), and the local stress of each grain σ_{ij} is continuously updated for all the grains using the self-consistent relation (8).

RESULTS AND DISCUSSION

The developed model has been applied to several superplastic aluminum alloys and comparisons are made with experimental data. In its present form, the model is applicable only to pseudo single phase materials because it considers all the grains to have the same elastic constants. We have chosen both statically recrystallized and dynamically recrystallizing aluminum superplastic alloys to study because they are the most widely used pseudo single phase superplastic materials. The first alloy is a fine grained, statically recrystallized 7475 aluminum alloy with a composition of 5.6 % Zn, 2.13 %Mg, 1.48 %Cu, 0.2 % Cr, 0.04 % Si, 0.02 % Ti, 0.01 % Mn, and the remainder being Al. Its superplastic deformation behavior has been reported by Hamilton et al. [6]. Flow stress vs. true strain rate curves have been obtained for this alloy by conducting uniaxial step strain rate change tests.

The aluminum alloys have a face-centered-cubic crystal structure with four {111} slip planes and three <110> slip directions on each plane, resulting in twelve slip systems in each grain. We consider the data at 644, 700 and 755 ^oK for the application of our model. For this range of temperatures, the average shear modulus μ is given as 20 GPa and the Poisson's ratio ν as 0.28 [7]. The elastic moduli affect only the elastic region of a stress-strain curve and they have virtually no effect on the flow stress. Therefore, small variations in elastic constants do not affect our calculations. Because of this reason and their structure insensitive nature, the same temperature-dependent elastic moduli have been assumed for all the aluminum alloys considered in this paper. The activation energy for lattice diffusion Q_L and that for grain-boundary diffusion Q_B have been obtained from the literature [8] as 142 KJ/mole and 84 KJ/mole respectively. These values do not change with alloying for pseudo single phase materials.

The incremental procedure given in the previous section is used to determine the stress-strain curves of the material at the various strain rates. For step strain rate change tests, the calculations are performed at a certain strain rate till a given strain is reached and then the strain rate is jumped up and the calculations are continued. Consider the experimental data at 700 ^oK. Appropriate values are chosen for the material constants a_l, a_b, a_s, and n and step strain rate change tests are simulated using the incremental procedure. We conduct the simulation at a certain strain rate until the stress vs. strain curve flattens out. The stress at this stage is the flow stress at that strain rate. Then, we increase the strain rate and continue the simulation until all the strain rates have been attained. The material constants that best fit this set of experimental data are $a_l = 1.4 \times 10^7$, $a_b = 3.74 \times 10^3$, $a_s = 9.2 \times 10^6$, and $n = 4$. The stress-strain curves obtained using these constants and the experimentally determined flow stress values are shown in Fig. 2. The agreement between the experiment and the simulation is seen to be quite good. The simulation and experimental data shown in Fig. 2 are represented in the form of a logarithmic plot of flow stress vs. strain rate in Fig. 3. Following the simulation, the flow stress vs. strain rate at two other temperatures 644 and 755 ^oK are *independently predicted.* This is done by merely providing the required temperature value in equations (3) and (4) and using the material constants obtained earlier. As it can be seen from Fig. 4, the predictions are good.

Next, we consider another statically recrystallized aluminum alloy Al-6Mg. Its composition is 5.8 % Mg, 0.37 %Zr, 0.07 % Cr, 0.16 % Mn, and the remainder being Al. Its superplastic deformation behavior has been reported by Matsuki et al. [9]. We consider the data at 703, 733 and 763 ^oK for the application of our model. The four material constants are obtained by simulation of the experimental data at 733 ^oK. They are $a_l = 1.73 \times 10^7$, $a_b = 9.34 \times 10^3$, $a_s = 5.5 \times 10^6$, and $n = 4$. The flow stress vs. strain rate obtained using these constants at the various strain rates and the corresponding experimental data points are shown in Fig. 6. With these parameters, we *independently predict* the flow stress vs. strain rate at the two other temperatures. Both experimental data and theoretical predictions are shown for these two temperatures in Fig. 7. The predictions appear to be quite good.

The next alloy we have considered is SUPRAL, which is a dynamically recrystallizing alloy. Its dynamic superplastic flow characteristics have been reported by Bricknell and Bentley [10]. It has a composition of 6.2 % Cu, 0.39 %Zr, 0.06 % Si, 0.06 % Fe, and the remainder being Al. The material constants have been obtained by simulation of the experimental data at 743 ^oK. They are $a_l = 1.43 \times 10^7$, $a_b = 3.0 \times 10^4$, $a_s = 1.0 \times 10^7$, and $n = 4$. The flow stress vs. strain rate obtained using these constants at the various strain rates and the corresponding experimental data points are shown in Fig. 8. With these parameters, we *independently predict* the stress vs. strain rate at two other temperatures 723 and 763 ^oK. Both experimental data and theoretical predictions are shown for these two temperatures in Fig. 9. The predictions appear to be good. Thus, we can see that our model is able to predict the superplastic behavior of both statically recrystallized and dynamically recrystallizing pseudo single phase aluminum alloys.

SUMMARY AND CONCLUSIONS

There is a need to understand the deformation mechanisms causing superplasticity both at low and at high strain rates. Preliminary study of microtexture using BKD technique shows that the contribution of diffusion, dislocation, and GBS mechanisms towards the superplastic deformation can be identified. A micromechanical model of superplastic deformation has been developed from the constituent grain level to the level of the polycrystalline aggregate in an explicit manner. The local stresses required in this model are obtained by using the self-consistent relation. The model is physically based, and in the present form takes diffusional and dislocation as the accommodation mechanisms. Other micromechanism based models can also be analyzed using the proposed technique. Material constants that determine the macroscopic superplastic strain from the accommodation strain are derived at one temperature and then the flow stress vs. strain rate behavior is predicted for different temperatures. Statically recrystallized 7475Al and dynamically recrystallizing SUPRAL alloys have been studied and the experimental observations match well with the theoretical predictions. The effect of grain size on SP deformation is presently being incorporated into the model. The ultimate goal of this research is to model high strain rate superplasticity and predict the presence or absence of superplasticity based on the composition, and the shape and distribution of the different phases in a material.

ACKNOWLEDGMENTS

This work was partially supported by the National Aeronautics and Space Administration and by the Supercomputing Center at Florida State University.

REFERENCES

1. T. G. Langdon, *Materials Science and Engineering*, A174, 225 (1994).
2. K. Murali and G. J. Weng, *Materials Science and Engineering*, A172, 43 (1993).
3. O. D. Sherby and J. Wadsworth, in *Superplasticity in Metals, Ceramics, and Intermetallics*, p. 3, Materials Research Society, Pittsburgh, PA, (1990).
4. J. Weertman, *Philosophical Magazine*, 11, 1217 (1965).
5. B. Budiansky and T. T. Wu, in *Proceedings, 4th U.S. National Congress of Applied Mechanics*, p. 1175, (1962).
6. C. H. Hamilton, C. C. Bampton, and N. E. Paton, in *Superplastic Forming of Structural Alloys*, p. 173, (1982).
7. M. K. Rao and A. K. Mukherjee, *Materials Science and Engineering*, 80, 181 (1986).
8. H. J. Frost and M. F. Ashby, *Deformation-Mechanism Maps*, Pergamon, U.K., (1982).
9. K. Matsuki, Y. Uetani, M. Yamada, and Y. Murakami, *Metal Science*, 10, 235 (1976).
10. R. H. Bricknell and A. P. Bentley, *Journal of Materials Science*, 14, 2547 (1979).

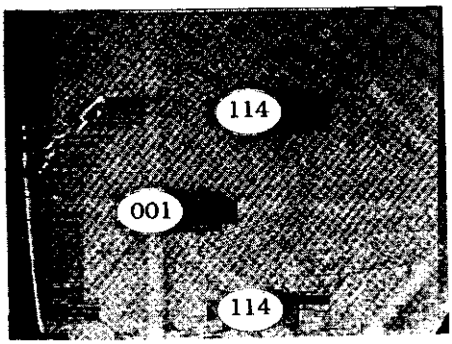

Fig. 1. A typical BKD pattern where the poles have been identified

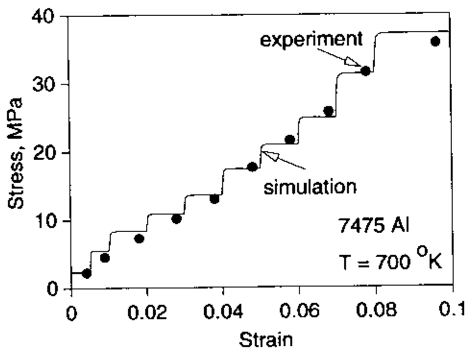

Fig. 2. Micromechanical theoretical simulation of the true tensile stress-true strain curve of 7475 aluminum alloy in a step strain rate change test

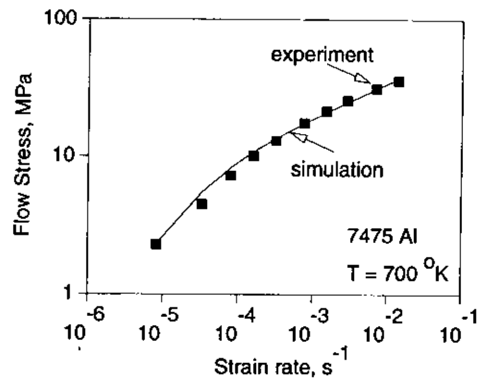

Fig. 3. Micromechanical theoretical simulation of the flow stress-true strain ratebehavior of 7475 Al

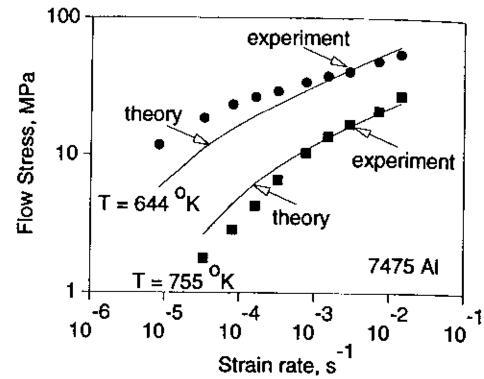

Fig. 4. *Independent prediction* of the flow stress-true strain rate behavior of 7475 Al

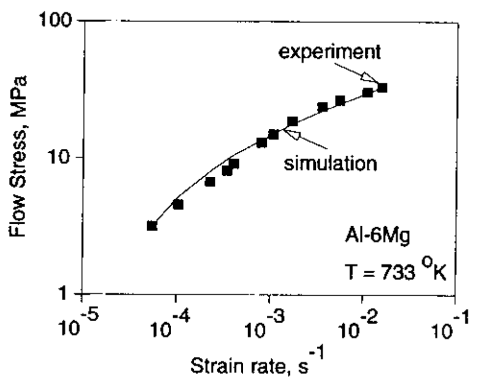

Fig. 5. Micromechanical theoretical simulation of the flow stress-true strain rate behavior of Al-6Mg

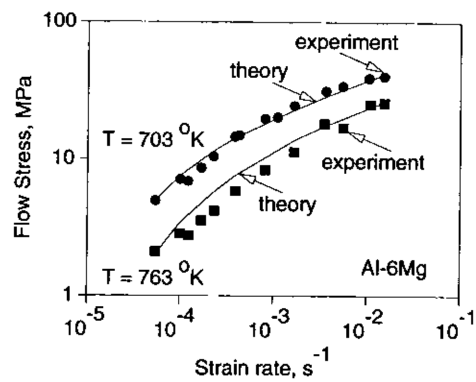

Fig. 6. *Independent prediction* of the flow stress-true strain rate behavior of Al-6Mg

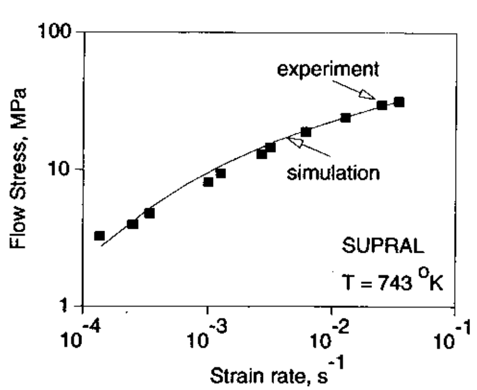

Fig. 7. Micromechanical theoretical simulation of the flow stress-true strain rate behavior of SUPRAL

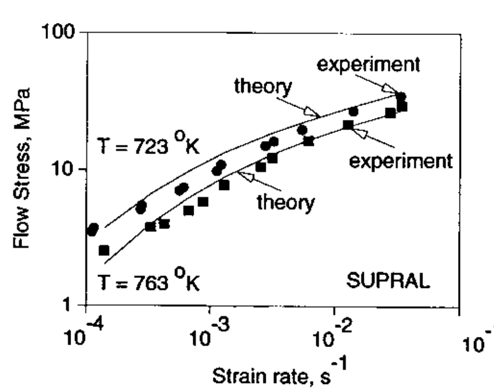

Fig. 8. *Independent prediction* of the flow stress-true strain rate behavior of SUPRAL